

N90-28649

## STRUCTURAL RESPONSE OF SSME TURBINE BLADE AIRFOILS

V. K. Arya, NRC Associate at NASA Lewis Research Center  
A. Abdul-Aziz, Severdrup Technology, Inc.  
R. L. Thompson, NASA Lewis Research Center  
Cleveland, Ohio

### ABSTRACT

Reusable space propulsion hot gas-path components are required to operate under severe thermal and mechanical loading conditions. These operating conditions produce elevated temperature and thermal transients which result in significant thermally induced inelastic strains, particularly, in the turbopump turbine blades. An inelastic analysis for this component may therefore be necessary. Anisotropic alloys such as MAR M-247 or PWA-1480 are being considered to meet the safety and durability requirements of this component.

An anisotropic inelastic structural analysis for an SSME fuel turbopump turbine blade was performed. The thermal loads used resulted from a transient heat transfer analysis of a turbine blade. A comparison of preliminary results from the elastic and inelastic analyses is presented.

### INTRODUCTION

Improved efficiency and durability are requirements of hot-gas path components of reusable space propulsion systems. These components are subjected to severe thermal and mechanical loads. These operating conditions result in severe thermal gradients and transients. These induce large inelastic strains and rapid crack initiation in the blade. Nickel-base superalloys are advantageous in such circumstances as they possess greater creep/fatigue resistance at elevated temperatures than the conventionally cast alloys. In polycrystalline turbine components, rupture is caused primarily by crack propagation originating at the grain boundaries. Since single crystal alloys like MAR M-247, Rene-N4, PWA 1480 etc., have no grain boundaries, their use in turbine components has significant advantages with regard to increased creep/fatigue resistance and longer service life. Assessing the life of turbine components like turbine blades (airfoils), is contingent upon an accurate description of their inelastic cyclic behavior. It is therefore necessary that sound analytical tools and realistic constitutive models be employed for predicting accurate deformation behavior, and thus the life span of these components.

The recognition of this need by the NASA Lewis Research Center has resulted in its launching a concerted effort to develop constitutive models and suitable numerical solution technologies capable of describing high-temperature inelastic behavior of single-crystal alloys. Viscoplastic constitutive models have been developed by Dame and Stouffer (1) and Walker and Jordan (2). These models include the interaction between creep and plasticity at high temperatures. They are based on a crystallographic approach to account for the different inelastic response of single-crystal materials from the polycrystalline nickel-base superalloys.

The mathematical framework of the above constitutive models is very complex. The constitutive equations are highly nonlinear and mathematically stiff. These considerations combined with the complex geometry and thermomechanical loadings

necessitate the use of numerical methods for the calculation of inelastic response and prediction of life of turbine blades.

The purpose of the present work is to perform the nonlinear finite element structural analysis of Space Shuttle Main Engine (SSME) blade. The crystallographic single-crystal viscoplastic model developed by Walker and Jordan (2) was selected to describe the inelastic response. The finite element program MARC (3) was employed to perform both the heat-transfer and structural analyses. The material of the blade is subjected to severe gas temperatures, and centrifugal and pressure loadings during the flight mission. Simulated mission cycle and loads used in the analyses are shown in Figure 1.

## ANALYSES

### FINITE ELEMENT MODEL

A three-dimensional, finite-element model of the airfoil (Fig. 1) was constructed of eight node, solid, isoparametric elements. This model, consisting of 360 elements with 576 nodes, was a shortened version of a finite element model created by Lockheed (4) for a NASTRAN steady-state analysis. The main difference between the NASA Lewis and Lockheed models was that the blade base and most of the platform were omitted for MARC heat transfer analysis in order to reduce the size of the problem as well as the computing cost for subsequent cyclic structural analyses. Analysis of the shank region was also hindered by lack of knowledge as to its thermal environment. The airfoil had a span length of 2.2 cm and a span-to-chord-width aspect ratio of approximately unity.

### HEAT-TRANSFER ANALYSIS

A boundary-layer analysis was conducted to compute the gas film coefficients needed for the heat transfer computation. The modified STAN5 (5) program was used to compute the boundary layer equations as well as the heat transfer coefficients. However, the leading edge of an airfoil poses a special problem for the STAN5 program in that a boundary layer profile is required and, therefore, to compute the heat transfer coefficients for the leading edge region, a correlation for local heat transfer on a cylinder in a laminar cross flow was used (6). This correlation is usually applicable only to laminar flow calculations for high speed gas turbines. However, to account for transitional effects into turbulence, an amplification term was selected from another correlation for the average heat transfer for a cylinder in cross flow (7).

Calculations of local values for the heat transfer coefficients at the leading edge stagnation region were implemented by modifying the correlation recommended by reference (6) with an amplification term where the effects of turbulence, angle variations and turbulent flow were accounted for. Details and a mathematical description of the correlations used in the heat transfer calculations may be found in reference (8).

The blade was assumed to operate at the steady-state portion of a full power cycle. The mission cycle consisted of a 4.5 sec transient from startup to steady-state, a 23.5 sec hold at steady-state and a 4 sec transient cutoff or shutdown. Rocketdyne provided the gas conditions from engine test data.

Transient boundary conditions for both heated and cooled surfaces along the airfoil, were scaled according to transient flow and temperature. The steady state heat transfer coefficients were adjusted by the ratio of the Reynolds number over the steady-state Reynolds number raised to the power of 0.8. This correlation is based on heat transfer coefficients along a flat plate. This means that the heat transfer coefficient is proportional to the power of 0.8 for turbulent flow.

Boundary conditions that reflect cooling by hydrogen fuel at the blade-to-disk attachment region were imposed by activating the MARC user subroutine FORCDT. The gas temperature was assumed to be constant over the airfoil surface at each time step. Boundary layer predictions at full power level conditions were input into the thermal model by means of MARC user subroutine FILM. Similarly, hot-gas temperature and Reynolds number histories were incorporated in the input.

## **STRUCTURAL ANALYSIS**

### **LINEAR (ELASTIC) ANALYSIS**

Single-crystal alloys display cubic symmetry in the elastic range. The elastic strain resulting from the lattice distortion is recoverable. The elastic stress-strain relationship can be uniquely described using three independent elastic constants namely, Young's modulus  $E$ , Poisson ratio  $\nu$ , and shear modulus  $G$ .

The elastic response of the airfoil was calculated using an eight node, brick element (compatible with the element used for the heat transfer analysis). The thermal and mechanical loads were applied incrementally to trace the simulated mission loading cycles (Fig. 1). The temperature values obtained from the heat transfer analysis were utilized in the calculations.

### **NONLINEAR (VISCOPLASTIC) ANALYSIS**

The nonlinear structural analysis of the airfoil is performed using the single crystal model developed by Walker and Jordan (2). The model is formulated by adopting a crystallographic slip theory and treats the inelastic response of the material to be anisotropic. To perform the finite element analysis, the model was implemented into the finite element program MARC. The user subroutine HYPELA in MARC program provides an efficient way to implement the constitutive equations. The material nonlinearity is incorporated into the finite element equilibrium equations through an initial load vector by treating it as a pseudobody force. An explicit self-adaptive time-integration strategy (9) is employed to integrate the constitutive equations. Because of the highly complex nature of the constitutive equations, the geometry of the blade, and thermomechanical loadings, some of the preliminary results from the viscoplastic analysis are presented. Complete results will be presented at a later date.

## **DISCUSSION OF RESULTS**

### **HEAT TRANSFER ANALYSIS**

Contour plots for metal temperature of the airfoil at different points during the cycle were generated. At 0.5 sec after startup, when the first ignition spike evaluated in the analysis occurred, the temperature gradient was essentially chordwise. The temperature tended to decrease until it reached the leading edge, where a significant

rise was observed. However, during this temperature spike, the temperature occurred at the trailing edge, particularly near the tip, where the airfoil was thinnest. At the second spike, 1.3 sec after startup, the maximum temperature was at the leading edge and that was expected because of high flow velocities which yielded high heat transfer coefficients in the region.

During cruise the airfoil experienced a uniform temperature distribution, except near the base, where a significant gradient is observed. This is due to the mixture of cold and hot gas in the area. At cutoff conditions, the heat transfer results demonstrated that the maximum temperature was always at the leading-edge. The trailing edge was a secondary high-temperature region. However, the temperature at the airfoil base region would have been lower if the platform and shank attachments were not simulated by boundary conditions.

Nevertheless, heat transfer results obtained were considered reasonable, although the scaling procedure used in the transient analysis did not fully account for the effects of boundary-layer history, or the blade heat capacitance in response to gas temperature. However, the significance of that on the stress analysis results may not be that great since the load barrier on the blade is not only thermal, it is high pressure and mechanical loads as well.

## **STRUCTURAL ANALYSIS**

### **ELASTIC ANALYSIS**

The elastic structural analysis for the airfoil has been completed for the complete simulated mission cycle (Fig. 1). The results at the points B, C, and D of the mission cycle for the temperature and elastic stress and strain distributions in the airfoil are shown in Figures 3 through 10. The stresses and strains shown in these contour plots are along the span of the airfoil. The strains plotted are the total (elastic + thermal) strains. The figures exhibit the temperature, stress and strain distributions on the pressure as well as the suction side of the airfoil. It is seen from these figures that the maximum stress (in magnitude) and strains occur in the blade after the first spike (point B of the mission cycle). During the cool-down to point C of the mission cycle, the stresses are reduced significantly in magnitude, and at point C, the whole airfoil is under compression. During the second spike, (point D of the mission cycle), the stresses and strains increase in magnitude again, and the whole airfoil is subjected to tension at D. The airfoil is thus subjected to severe loading conditions going repeatedly from tension to compression and vice-versa.

For an accurate life analysis of structural components subjected to such severe loadings, it is necessary to perform the inelastic (viscoplastic) structural analysis. The viscoplastic analysis for the airfoil is in progress. Because of the severity of the problem caused by complex geometry and complex thermomechanical loadings, only preliminary results using the single-crystal viscoplastic model for PWA 1480 have been obtained so far.

### **VISCOPLASTIC ANALYSIS**

The results for stress and strain distributions in the airfoil obtained using Walker and Jordan's model (2) are shown in Figures 12 and 13. The time is 0.6 sec (first spike) and the temperature distribution is shown in Figure 11. The stresses and total strains plotted in these figures are again those along the span of the airfoil. The magnitudes of stresses and strains from the viscoplastic analysis are slightly different

(slightly higher) than those from the inelastic analysis. This may possibly be due to the slightly different approaches adopted for the calculations in the two analyses. The main point is that even with these preliminary and crude (because of a large time-step size), the results demonstrate the feasibility of performing the viscoplastic analysis for this complicated problem.

## FUTURE WORK

The viscoplastic analysis for the SSME-airfoil for the complete simulated flight mission cycle is underway. The results of this analysis will be presented at a later date. It is proposed to predict the life of airfoil by employing the results from the viscoplastic analysis. It is expected that the results will aid in improved design of the SSME turbopump blade airfoil.

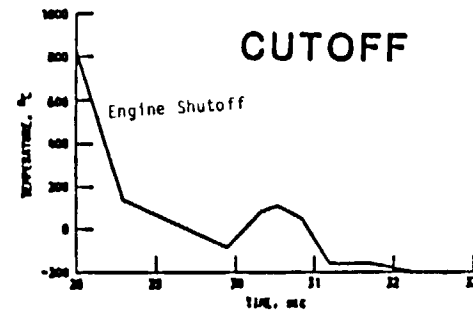
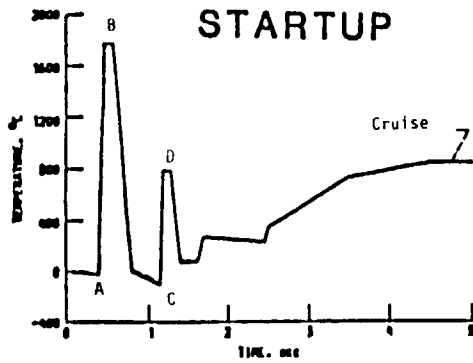
## REFERENCES

1. Dame, L.T. and Stouffer, D.C.: Anisotropic Constitutive Model for Nickel Base Single Crystal Alloys : Development and Finite Element Implementation. NASA CR-175015, 1986.
2. Walker, K.P. and Jordan, E.H.: Biaxial Constitutive Modeling and Testing of a Single Crystal Superalloy. To appear in Fatigue of Engineering Materials and Structures, 1988.
3. MARC General Purpose Finite Element Analysis Program. MARC Analysis Research Corporation, Palo Alto, CA, 1983.
4. Hammet, J. C., et al.: Space Shuttle Main Engine, Powerhead Structural Modeling, Stress and Fatigue Life Analysis. Lockheed Missiles & Space Company; Huntsville Research & Engineering Center, NASA Contract NAS8-34978, NASA CR-170999, 1983.
5. R. E. Gaugler, " Some Modification to, and OPERational Experiences With, The Two-Dimensional, Finite-Difference, Boundary-Layer Code, STAN5 ". NASA TM-81631, 1981.
6. Martinelli, R. C., Guibert, A. G., Morrin, E. H., and Boelter, L.M.K, " An Investigation of Aircraft Heaters VIII- A Simplified Method for Calculation of the Unit Thermal Conductance Over Wings ". NACA Wartime Report, ARR WR-W-14, MAR. 1943.
7. Churchill, S. W. and Bernstein, M., " A Correlating Equation for Forced Convection from Gases and Liquids to a Circular Cylinder in crossflow ". Transaction of ASME, Journal of Heat TRansfer, Vol. 99, May 1977.
8. Abdul-Aziz, A., Tong M., and Kaufman A.: "Thermal Finite-Element Analysis of SSME Turbine Blade ". NASA TM-1000117, 1987.
9. Arya, V.K.; Hornberger, K. and Stamm, H.: On the Numerical Integration of Viscoplastic Models. Report No. KfK-4082,

Kernforschungszentrum Karlsruhe, West Germany, 1985.

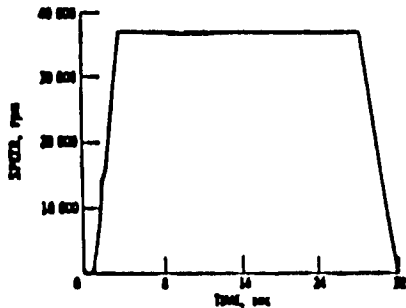
# MISSION CYCLE

- 1- Point A (0.41 sec after startup)
- 2- Point B (0.5 sec after startup)
- 3- Point C (1.14 sec after startup)
- 4- Point D (1.2 sec after startup)
- 5- Cruise
- 6- Engine Shutoff

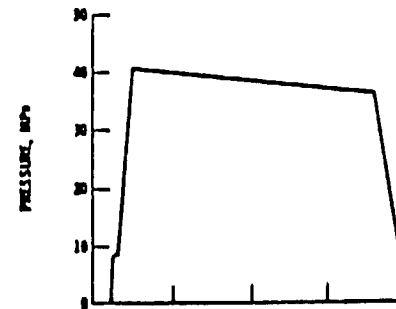


## TURBINE INLET GAS TEMPERATURE

FIGURE - 1



BLADE SPEED



TURBINE INLET PRESSURE

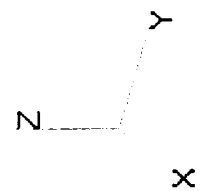
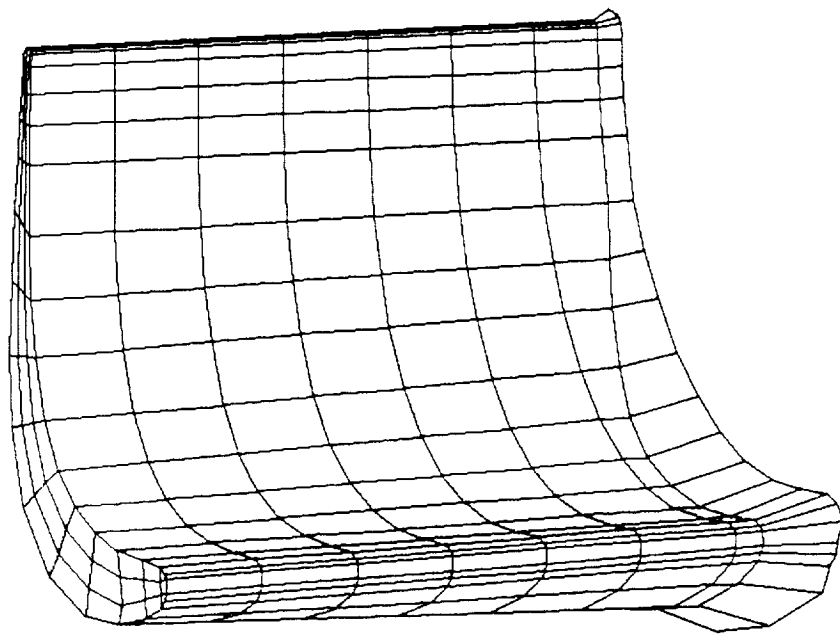


FIG. 2 - AIRFOIL FINITE ELEMENT MODEL  
(360 ELEMENTS, 576 NODES)



FIG. 3 - TEMPERATURE DISTRIBUTIONS OF SSME-BLADE AIRFOIL

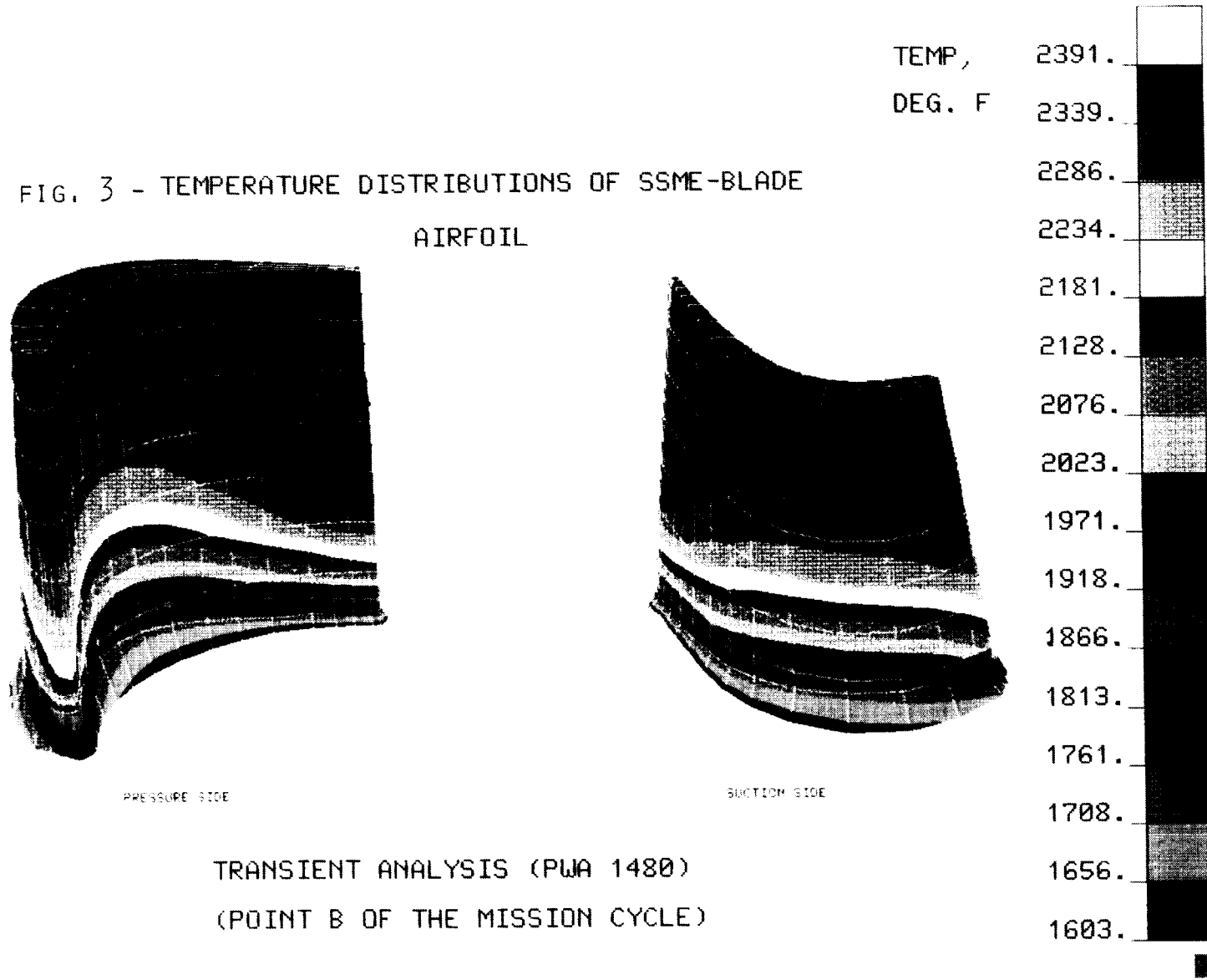
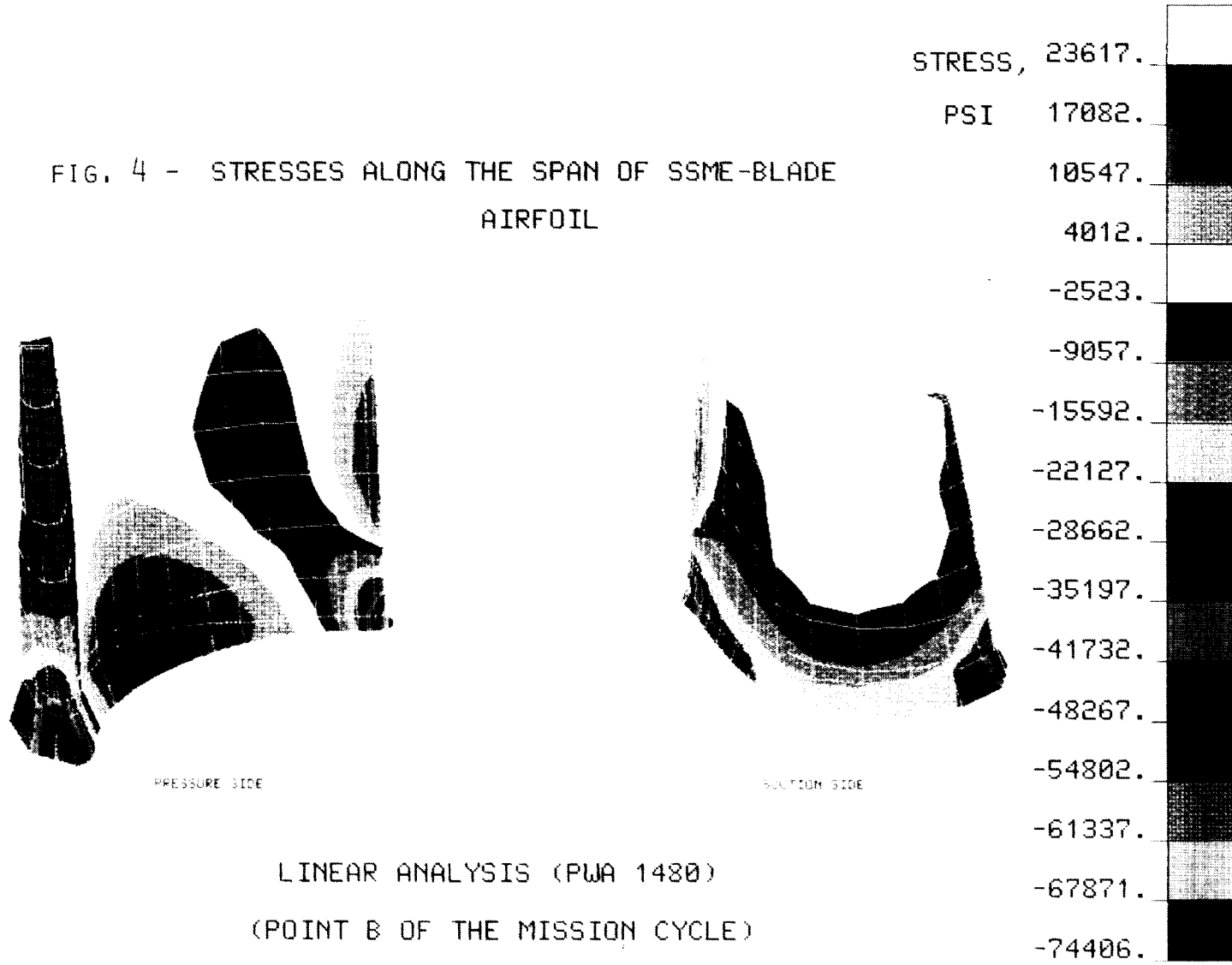


FIG. 4 - STRESSES ALONG THE SPAN OF SSME-BLADE AIRFOIL



LINEAR ANALYSIS (PWA 1480)  
(POINT B OF THE MISSION CYCLE)

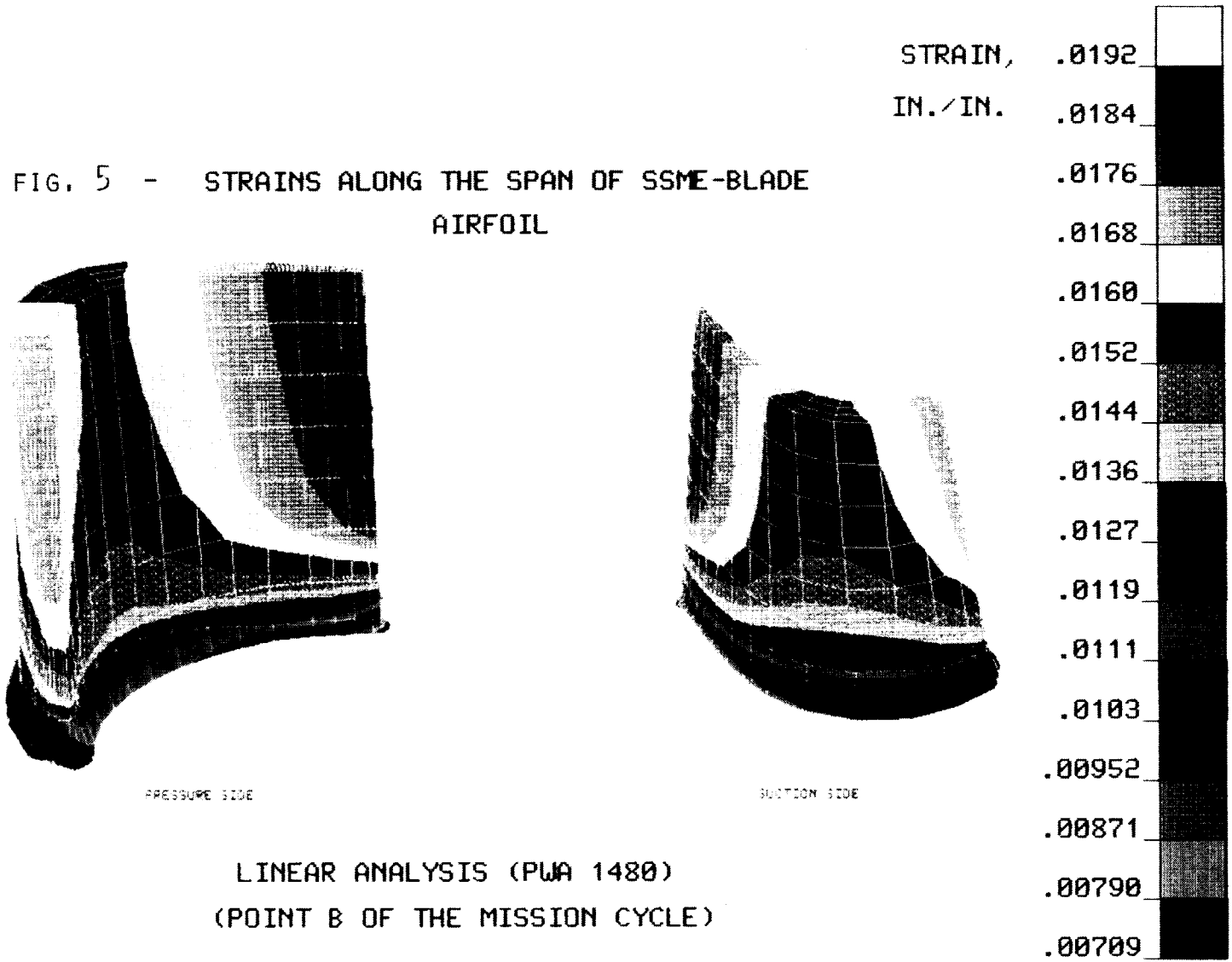
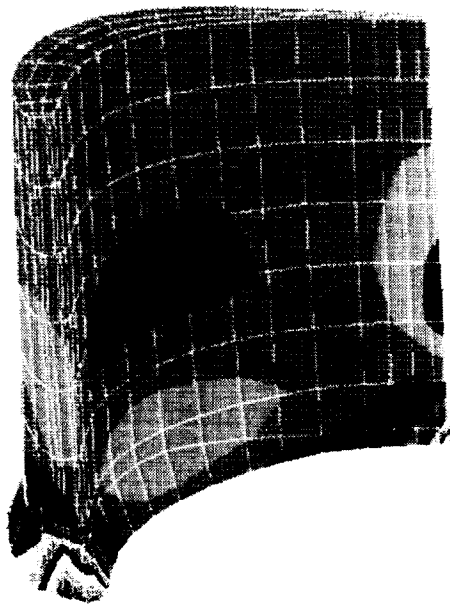
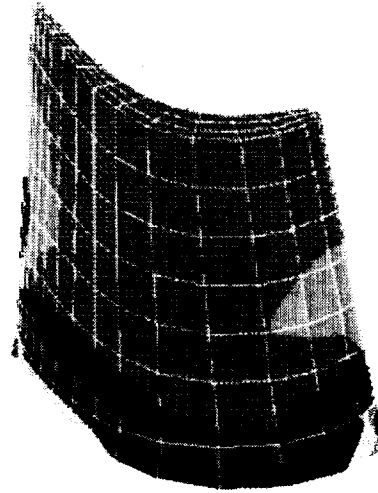


FIG. 6 - STRESSES ALONG THE SPAN OF SSME-BLADE AIRFOIL



PRESSURE SIDE



SUCTION SIDE

STRESS,  
PSI

2936.  
2703.  
2469.  
2235.  
2002.  
1768.  
1534.  
1300.  
1067.  
833.  
599.  
365.  
132.  
-102.  
-336.  
-570.



LINEAR ANALYSIS (PWA 1480)  
(POINT C OF THE MISSION CYCLE)

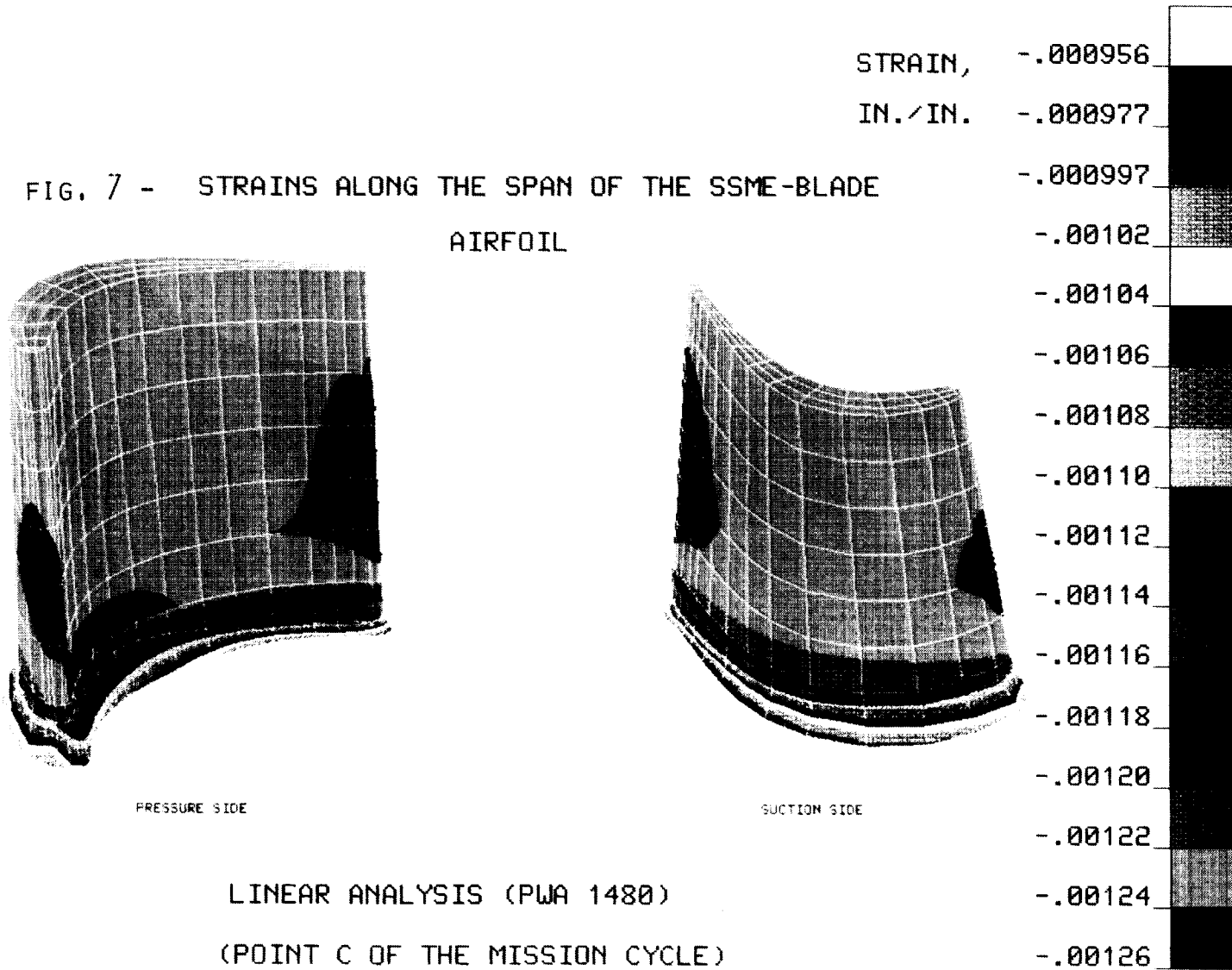
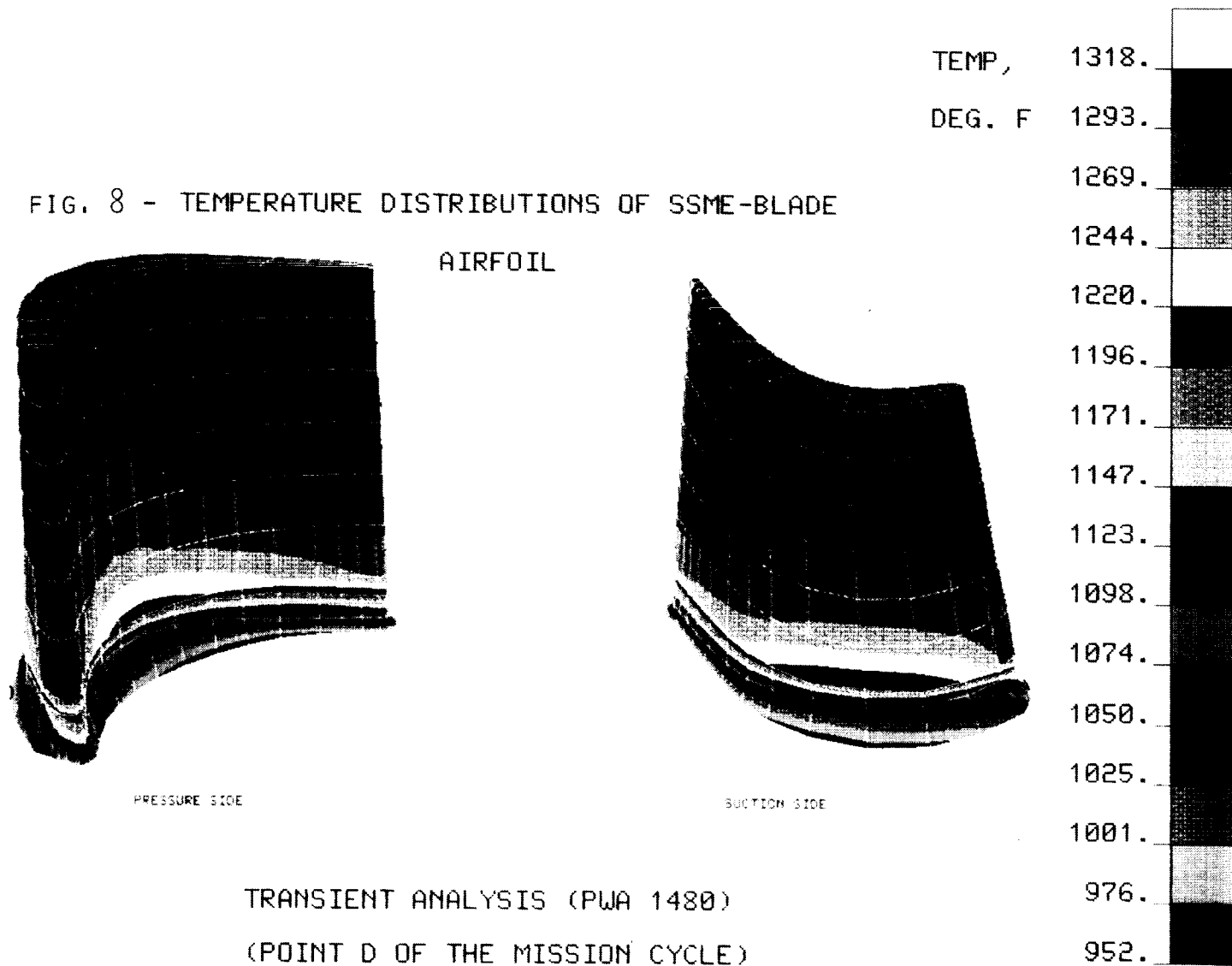


FIG. 8 - TEMPERATURE DISTRIBUTIONS OF SSME-BLADE



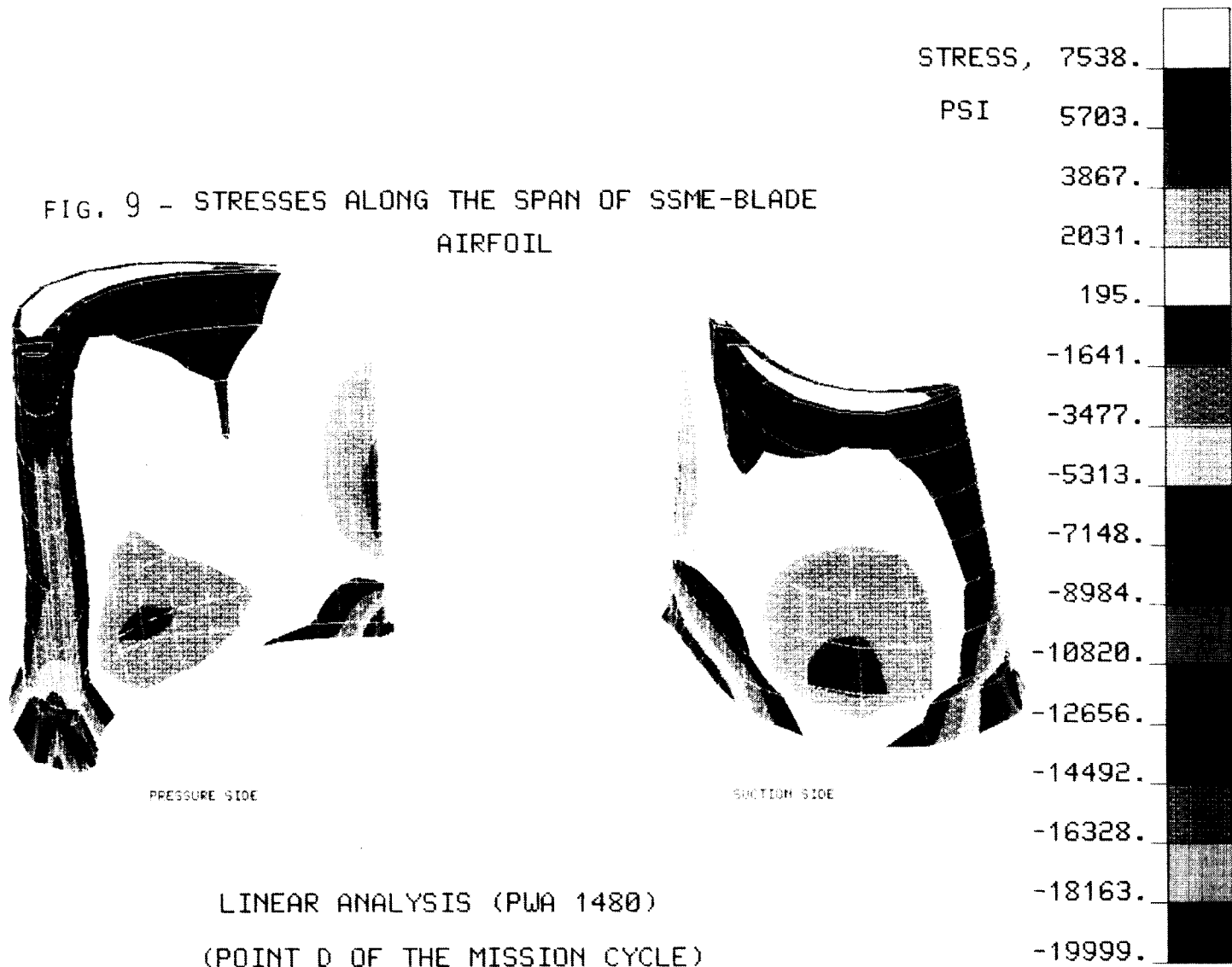
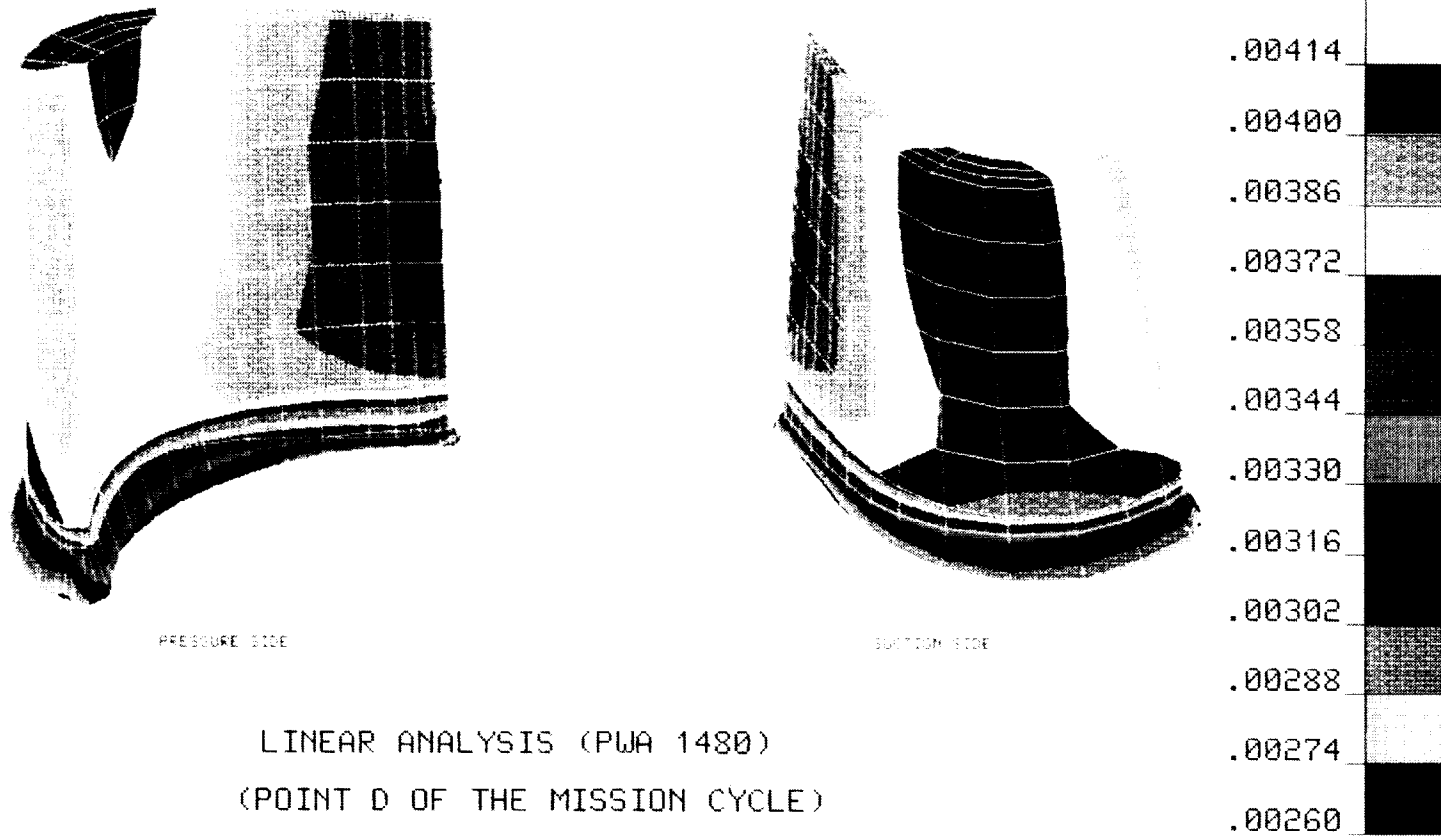


FIG. 10 - STRAINS ALONG THE SPAN OF SSME-BLADE AIRFOIL



LINEAR ANALYSIS (PWA 1480)  
(POINT D OF THE MISSION CYCLE)



FIG. 11 - TEMPERATURE DISTRIBUTION IN THE SSME-BLADE

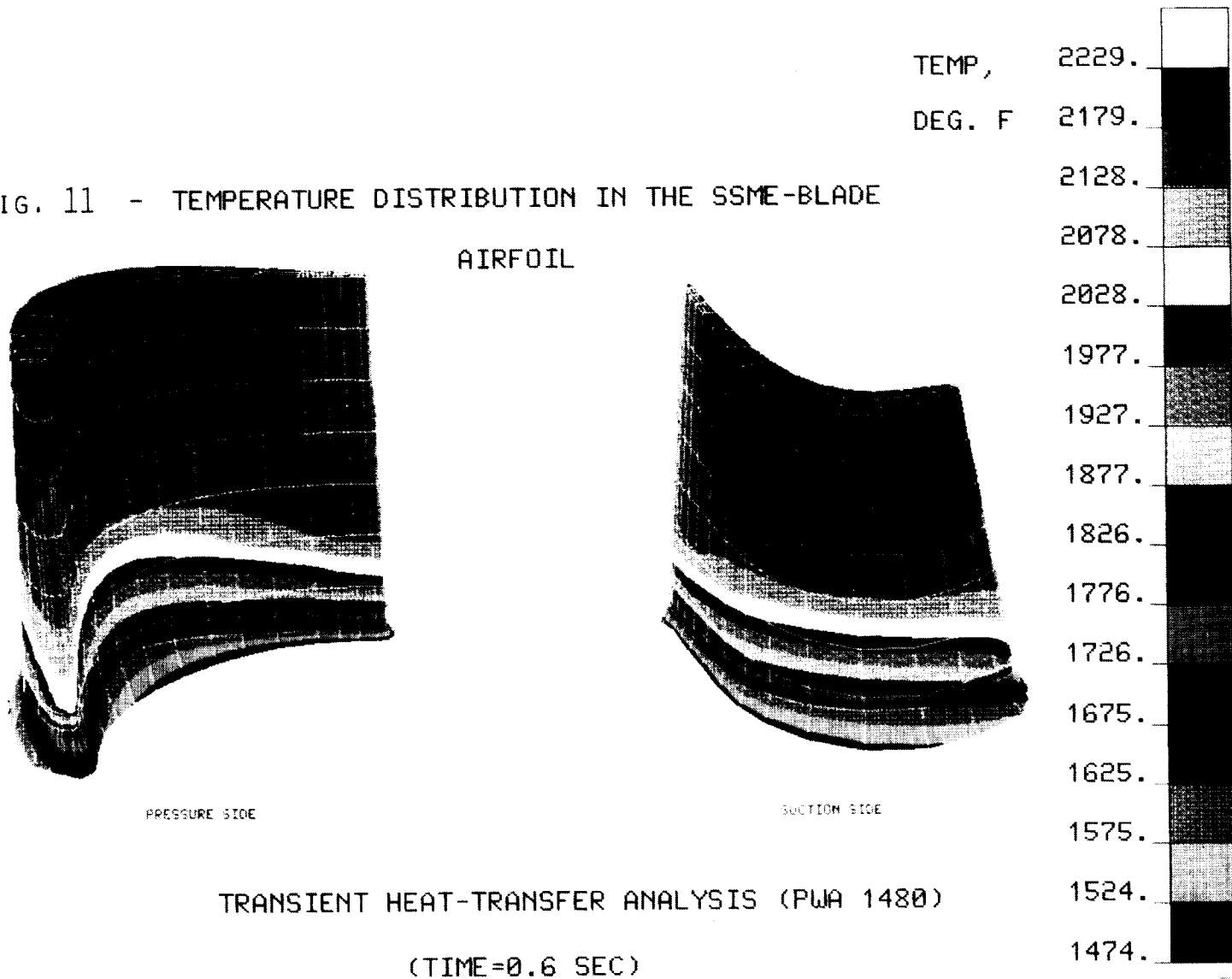


FIG. 12 - STRESSES ALONG THE SPAN OF THE SSME-BLADE AIRFOIL

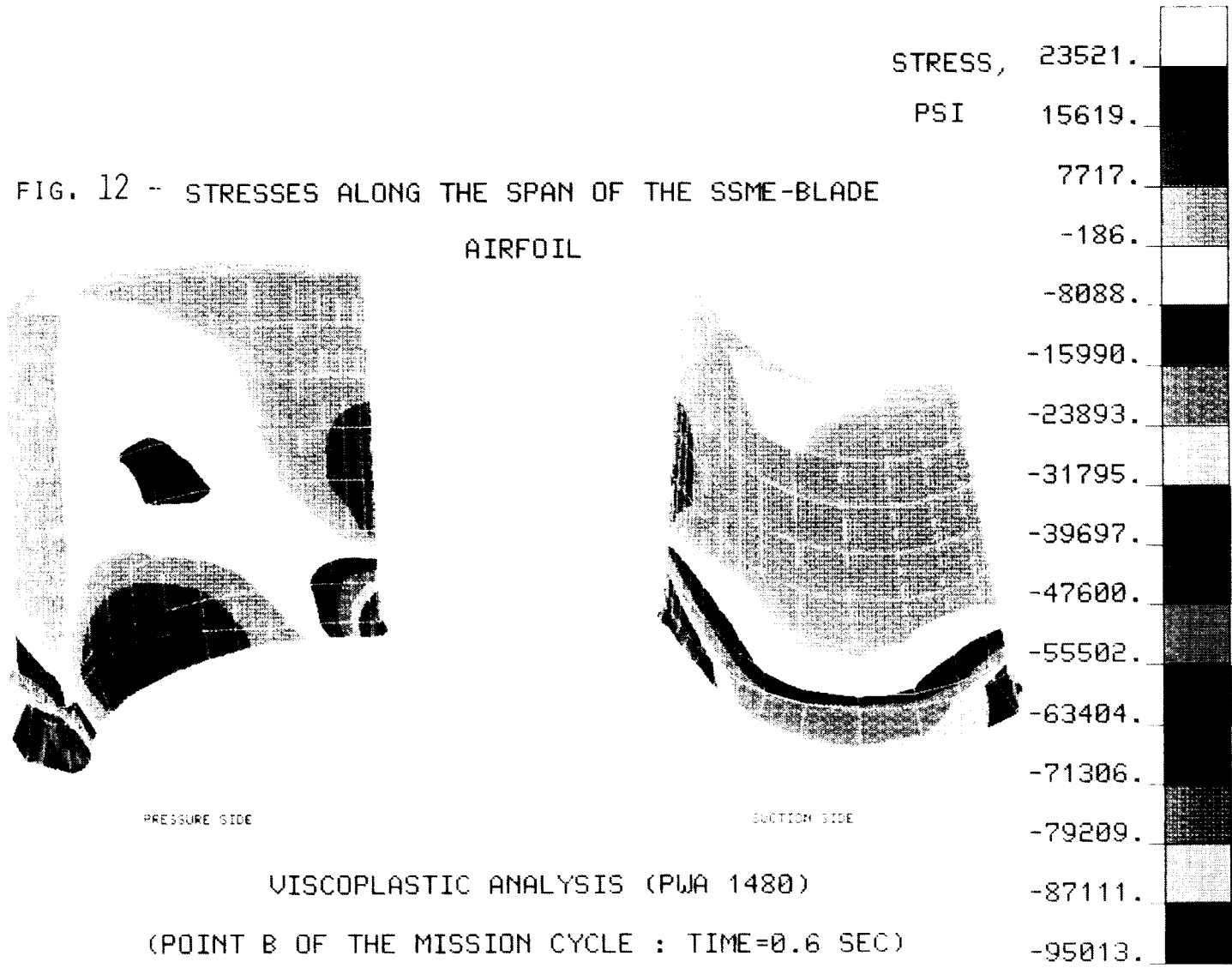


FIG. 13 - STRAINS ALONG THE SPAN OF THE SSME-BLADE

